United States Department of the Interior

Geological Survey

SUB-SEA TEMPERATURES AND A SIMPLE TENTATIVE MODEL FOR OFFSHORE PERMAFROST AT PRUDHOE BAY, ALASKA

by

Arthur H. Lachenbruch and B. Vaughn Marshall

Open-File Report 77-395

April 1977

This report is preliminary and has not been edited or reviewed for conformity with Geological Survey standards and nomenclature.

Contents

INTRODUCTION

In this report, we present temperatures measured in three holes drilled into the sea bed in the Prudhoe Bay region and a tentative interpretation of them in terms of the gross thermal regime and shoreline history of the area. The new holes (PB-1, PB-2, and PB-3, Figure 1) were drilled in spring, 1976 (see Sellmann, 1976) as part of a cooperative study of off-shore permafrost by the USGS, CRREL, and the University of Alaska. Results from two of the holes (#190 and #3370, Figure 1) drilled earlier by the University of Alaska (Osterkamp and Harrison, 1976) have been included in our interpretation.

The reader not interested in analytical details may wish to examine Figures 1, 2, and 3, and then skip to the concluding section "Summary and Discussion," page 32.

ACKNOWLEDGMENT

This study was supported by the Bureau of Land Management through interagency agreement with the National Oceanic and Atmospheric Administration, under which a multi-year program responding to needs of petroleum development of the Alaskan continental shelf is managed by the Outer Continental Shelf Environmental Assessment Program (OCSEAP) Office.

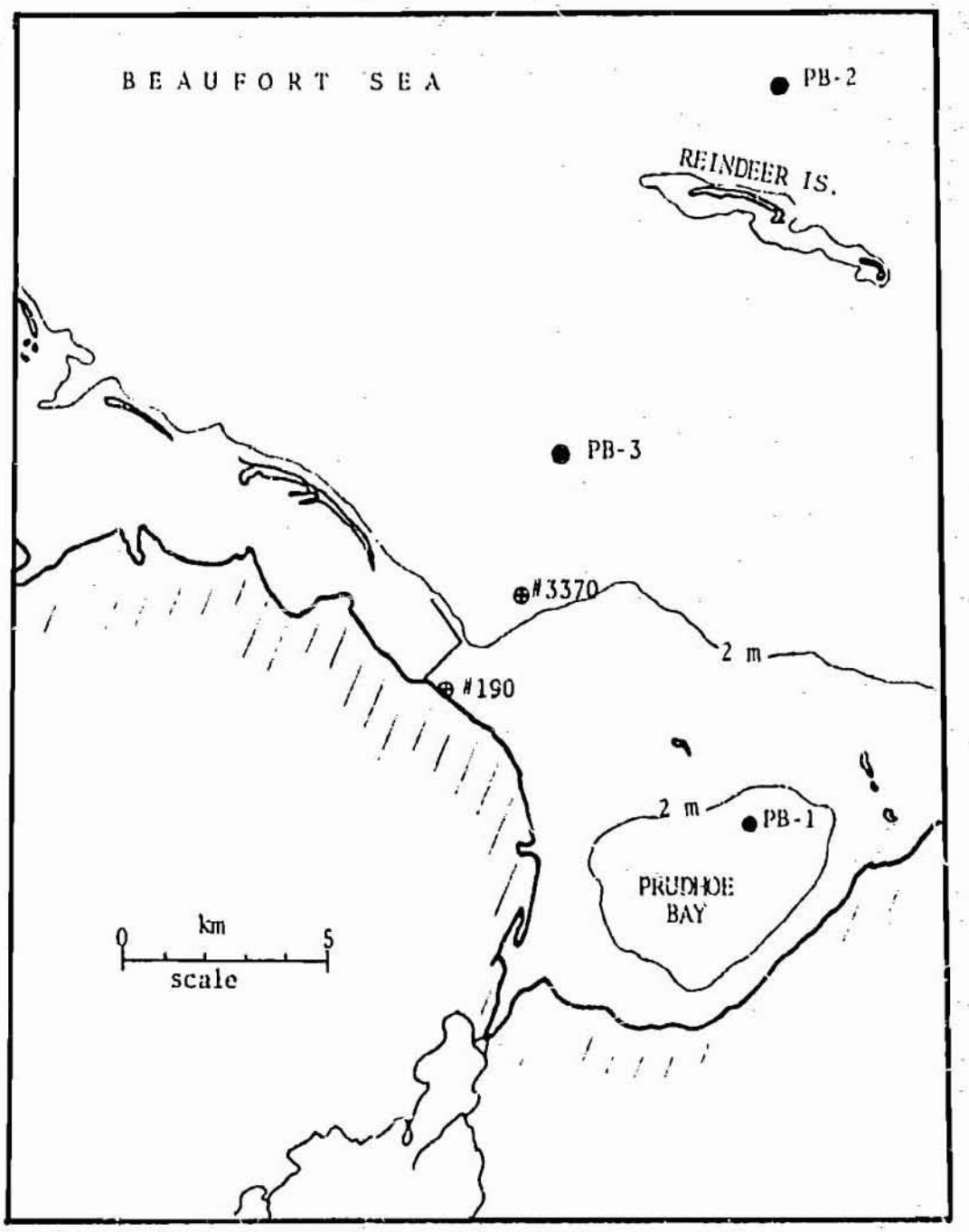

Figure 1. Map showing hole locations.

TEMPERATURE OBSERVATIONS

Temperature measurements were made by logging from the surface with the "portable mode" of instrumentation described by Sass and others (1971). Equilibrium observations were made to millidegree precision at discrete depth increments of about 1 meter. The time constant for the temperature transducer is only a few seconds, and the measurement accuracy of the system is probably a few hundredths of a centigrade degree. The observational data are presented in tabular form in the Appendix. Pre-drilling temperatures estimated for selected depths by the method of Lachenbruch and Brewer (1957) are shown with temperatures from the two University of Alaska holes in Figure 2. More refined estimates of the equilibrium temperature will be undertaken at a later date, but the results shown are adequate for the present purpose.

The line of holes drilled by the University of Alaska extends 3.37 km outward from the shoreline to a point where about 0.8 m of sea water occurs under the 2 m of ice that forms seasonally (see inset, Figure 2). Holes PB-3 and PB-2 extend that line seaward. PB-3 is 6.62 km from the shore where the combined water and ice depth is 5.8 m, and PB-2 is 17.0 km from shore beneath 11.6 m of water and ice. Conditions at PB-2 are complicated by proximity to Reindeer Island, a barrier island whose position is probably changing with time (see e.g., Hopkins and others, 1977). Hole PB-1 lies within Prudhoe Bay proper, about 3 km from the shoreline; 0.7 m of sea water underlies the 2 meters of seasonal

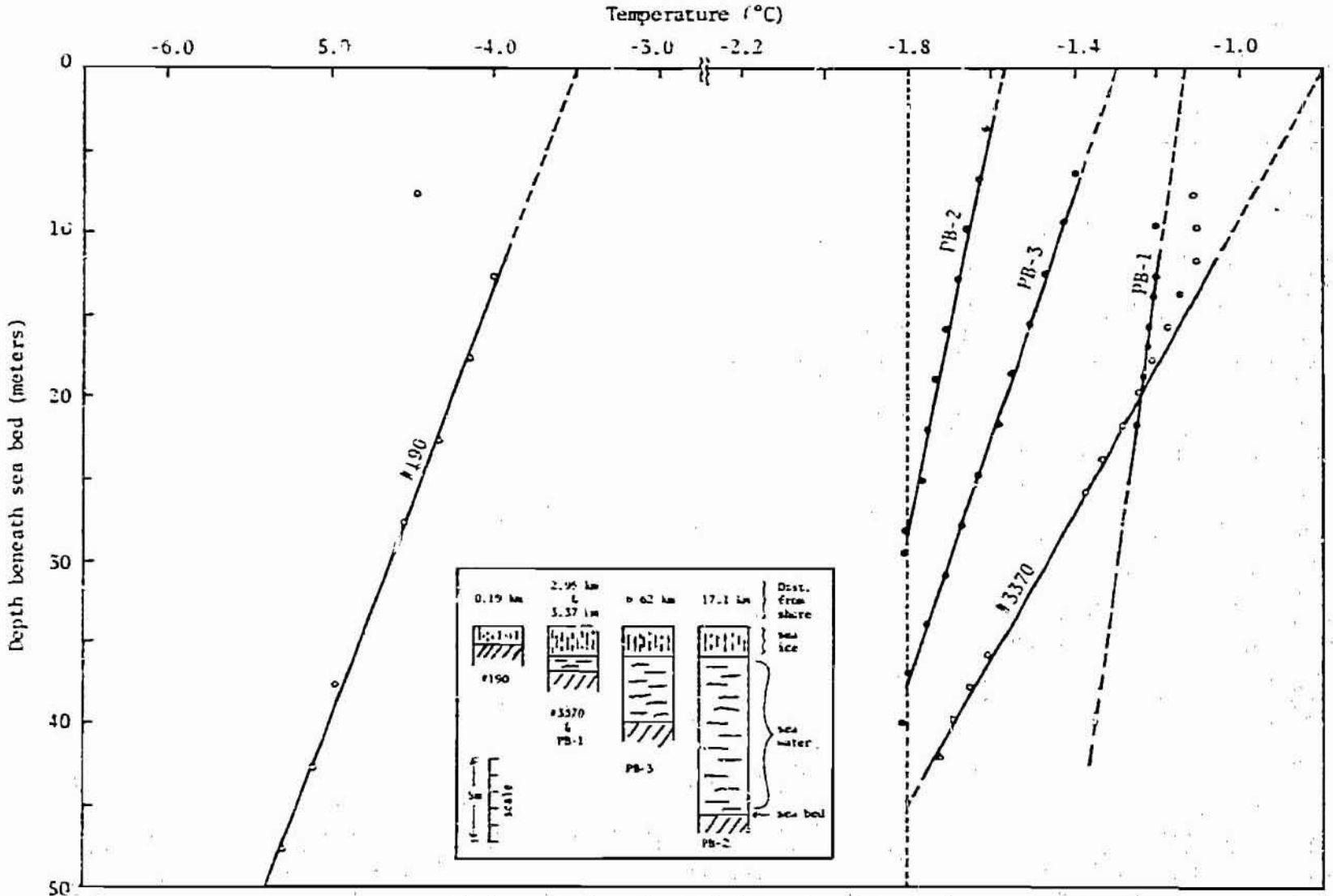

Figure 2. Estimated pre-drilling temperatures beneath sea bed for five ho` in Prudhoe Bay area. (Open circles from Osterkamp and Harrison, 1976.) Inset shows distance from .sent shoreline and depth of sea water and seasonal ice. (Note change in temperature scale at -3.0 °C.)

ice there. Table 1 lists other information about these three holes and two of the holes (#190 and #3370) drilled by the University of Alaska and discussed by Osterkamp and Harrison (1976).

Insofar as is known, no frozen material was penetrated by holes PB-1, PB-2, and PB-3 or by hole #3370 (Osterkamp and Harrison, 1976). This is consistent with the general linearity of temperature profiles in the lower parts of these holes (Figure 2) which implies steady-state conduction in homogeneous materials with no phase changes in progress. However, the uncertain bottom-most points on profiles PB-2 and PB-3 (Figure 2) suggest a sharp decrease in gradient; they may represent a transition at the bottom of each hole to thermal conditions in ice-bonded permafrost.) Hole 190 evidently penetrates relatively homogeneous ice-bonded material (Osterkamp and Harrison, 1976). Holes PB-3, PB-2, and 3370 were all terminated because of drilling difficulties at or near the depth of the -1.8°C isotherm (Figure 2). As -1.8°C is the approximate freezing temperature of normal sea water, this observation suggests that the reason the drilling became difficult at these depths was because ice-bonded permafrost was encountered there, and that the thawed sediments penetrated were saturated with normal sea water.

This important observation provides evidence for the temperature, Θ_f, of the top boundary of ice-bonded permafrost at these localities. This boundary temperature is determined by the freezing temperature (and consequently the salinity) of interstitial water in the sediments

TABLE 1. Data for 5 offshore boreholes, Prudhoe Bay

								Deposition D							
(1)	(2)	(3)	(4)	(5)	(6)	(7)	(8)	(9)	(10)	(11)	(12)	(13)	(14)	(15)	(16)
Hole	Distance from shore (m)	Ice + water (m)	θ_o (°C)	θ_f (°C)	ϵ (°C)	X (m)	$\frac{L}{2k_s}\frac{X^2}{c}$ (yrs)	Marine (m)	$\frac{1}{2}\lambda$ Beach (m)	Total D (m)	$\frac{D}{X}$ (%)	$\frac{Q_f(t)}{L\lambda}$ (%)	Total correction factor	t (yrs)	B-X' (m)
190	190	1.1	-3.5	?		-								(145)	~ 0
PB-1	2,950	2.7	-1.13	(-1.8?)	.67	(80?)	(11,030)	3.2	1.9	5.1	-(6%)		1.24	(13,600)	
3370	3,370	2.8	-0.8	-1.8	1.0	45	2,340	3.2	1.5	4.7	- 10%	54%	1.44	3,370	19 m
PB 3	3,620	5.8	-1.3	-1.8	0.5	37.5	3,250	4.8	2.4	7.2	- 19%	63%	1.44	4,660	29 m
PB-2	17,100	11.6	-1.57	-1.8	0.23	28	3,940	9.1	1.5	10.6	- 38%	80%	1.43	5,610	37 m

1) Columns 4-7 are inferences from observations.
2) Columns 8 and 12-14 refer to equation 13.
3) Columns 9, 10, 11 are estimates by David Hopkins.
4) Column 13 determined from equation 31.
5) Column 14 is the "correction" for column 8, see equation 13.
6) Column 15, effective time since inundation, determined from equation 35b for hole 190 and from equation 13 for others.
7) Column 16 determined from equations 44a and 48; for Prudhoe Bay B = 600 km.

contacting the ice-bonded interface. In principle, Θ_f can lie anywhere between 0°C and the eutectic temperature for sea water (about -23°C). Harrison and Osterkamp (1976) have emphasized that the actual value of Θ_f depends upon processes by which salt might be concentrated or trapped in the sea bed (e.g., by exclusion from freezing sea ice) and transported downward through the thawed sediments. They have shown that if the salt were transferred exclusively by diffusion, salinity would decrease sharply from the sea bed to the ice-bonded interface. If the salinity at the sea bottom were close to that of normal sea water (as it probably is in general when the water depth is substantially greater than ice thickness) the salinity gradient in the thawed layer would result in relatively fresh interstitial water at depth and higher values of Θ_f than inferred above. The rate of degradation of ice-bonded permafrost, and in fact whether or not degradation occurs, is very sensitive to small changes in Θ_f relative to the mean annual sea bed temperature, Θ_o.

The best estimate of the mean annual sea bed temperature Θ_o is obtained by upward extrapolation of the linear portion of the curves shown in Figure 2. The values so obtained are listed in Table 1, column 4. The values of Θ_o for the four sites where the water depth is at least 3 m or so, vary from -0.8°C closest to shore to -1.57°C at the site farthest from shore. If Θ_f were not less than Θ_o, there would be no progressive thawing from one year to the next and the ice-bonded permafrost would persist close to the sea bed. As Osterkamp and Harrison (1976) have pointed out, this is evidently the case at hole #190 which

is typical of the near-shore region in which ice freezes to the sea bed annually. Here conductive cooling in the winter reduces the mean annual temperature, Θ_o, to about -3.0°C which is probably less than the freezing temperature of interstitial water, except possibly for effects of seasonal salt concentrations. Thus within the near-shore band of grounded sea ice, it is likely that $\Theta_f > \Theta_o$, and ice-bonded permafrost can persist close to the sea bed. It is important to emphasize that were it not for effective salt transport through surficial sediments at the other sites, this condition ($\Theta_f > \Theta_o$) could obtain also in the deeper water. As Osterkamp (1975) and Harrison and Osterkamp (1976) have stressed, the parameters controlling this salt transport process must be understood before we can predict whether or not ice-bonded permafrost is likely to occur close to the sea bed. If the salt is transported primarily by movement of interstitial water, it will be important also to confirm that the heat transport is primarily conductive as is generally assumed.

A SIMPLE "TARGET" MODEL FOR PRUDHOE BAY PERMAFROST

Recognizing the hazards of premature generalization, we feel that at this time it is useful to construct a highly idealized preliminary model of the gross features of Prudhoe Bay permafrost. Although it will certainly be wrong in detail, it should serve to focus attention on the sensitive parameters and provide some guiding context for future work. It is a target model in the sense that it gives us something to "shoot" at. With this introduction we shall not further belabor the presentation with cautious qualifying remarks. A more rigorous synthesis will be presented with onshore data from the region after the completion of the 1977 fieldwork. For the most part, the following discussion is based upon well known results from heat-conduction theory and concepts that have been stated or implied in work published over the last 25 years (Terzaghi, 1952; Lachenbruch, 1957; Carslaw and Jaeger, 1959, chapter XI; Lachenbruch and others, 1962, 1966; Mackay, 1972; Gold and Lachenbruch, 1973; Sharbatyan and Shumskiy, 1974; Osterkamp, 1975; Hunter and others, 1976; Osterkamp and Harrison, 1976; Harrison and others, 1977).

The model is represented schematically in Figure 3. At the time of submergence the temperature is given by the curve t=0; thereafter the sea bottom is maintained at temperature Θ_o, and the melting (and freezing) temperature of interstitial ice is maintained at Θ_f at the upper surface and Θ_f' at the lower surface of the ice-bonded permafrost. We shall assume that Θ_o and Θ_f have remained constant at their presently observed values since some effective date of submergence t=0. This, of course,

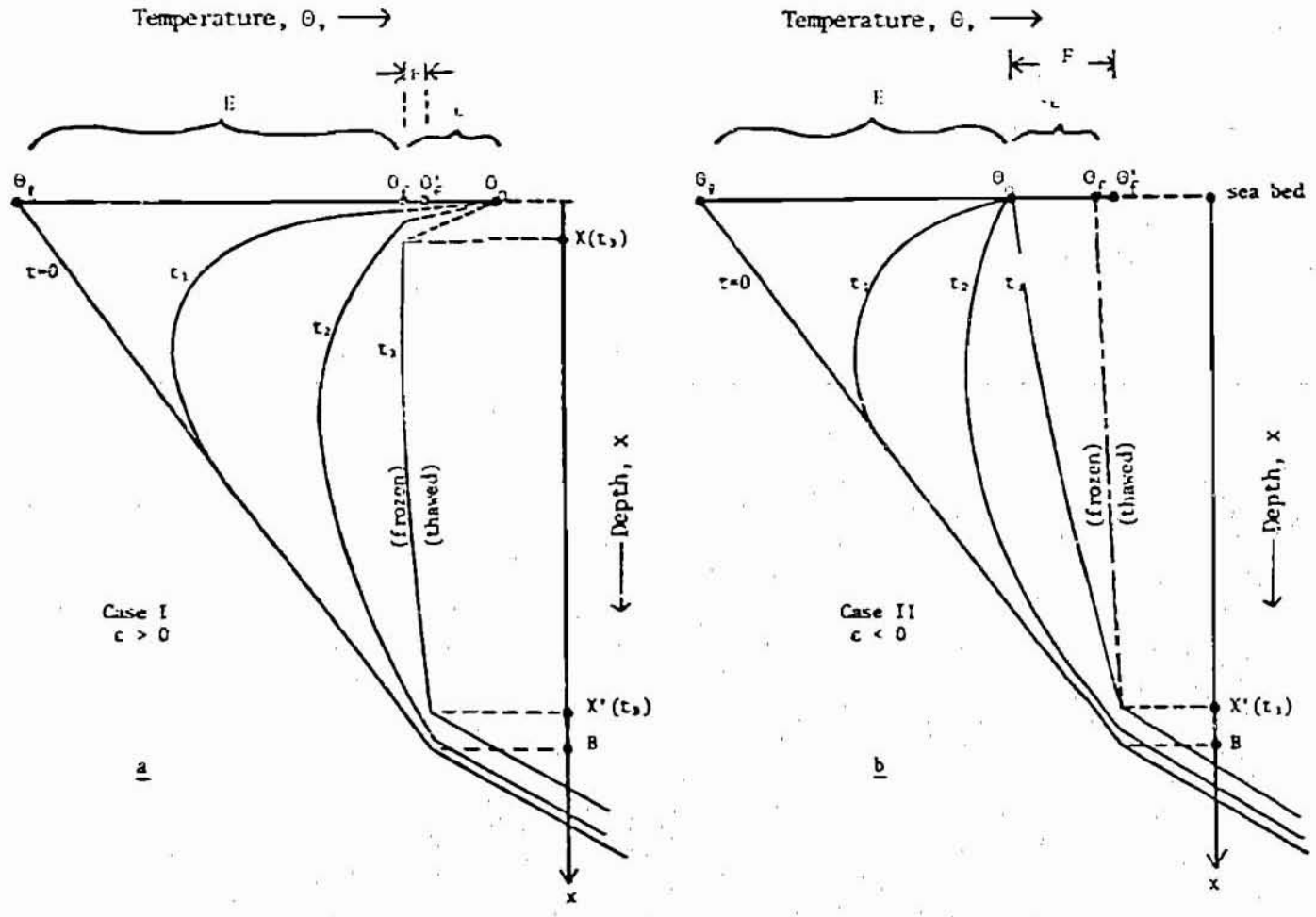

Figure 3. Schematic representation of sub-sea temperatures at successive times t=0, t_1, t_2, t_3, following submergence of a region underlain by ice-rich permafrost. a. Mean sea-bed temperature, Θ_o, greater than melting temperature, Θ_f, at top, X(t), of permafrost.

b. Mean sea-bed temperature, Θ_o, less than melting temperature, Θ_f, at top of permafrost.

cannot be true, but the assumption is justified by the resulting simplicity of the analysis and by our present ignorance of the time-dependence of these quantities. Figure 3a represents the case $\Theta_o > \Theta_f$ which results in a thawed layer at the sea bed (e.g., at holes 3374, PB-1, PB-2, and PB-3) and Figure 3b represents $\Theta_o < \Theta_f$ where there is only superficial thawing, resulting largely from seasonal effects (e.g., hole #190). The model is one-dimensional, i.e., we neglect horizontal transfer of heat, treating the submergence as if it were a sudden climatic change. For slow transgression and at points close to the shoreline, this assumption must be examined carefully. We assume further that essentially all of the latent heat is released over a very small temperature interval, effectively at Θ_f near the top of the ice-bonded permafrost, and at Θ_f' near the bottom of permafrost. We assume also that prior to submergence, a thermal steady state had been established on land, the geothermal flux, q^*, is constant and the thermal properties of the frozen (subscript "f") and thawed (subscript "t") materials are each uniform. The moisture content is assumed to be uniform also. These latter assumptions are reasonably consistent with subsurface observations on land near Prudhoe Bay.

Definitions of quantities in the analysis are as follows:

B initial depth of permafrost (on land).

Θ_ℓ long-term mean annual temperature at land surface (prior to submergence)

Θ_f freezing (and melting) temperature at top of ice-bonded permafrost

Θ'_f freezing (and melting) temperature at bottom of ice-bonded permafrost

Θ_o long-term mean annual temperature of sea bed at site of interest

ε $= \Theta_o - \Theta_f$

E $= \Theta_f - \Theta_\ell$ or $\Theta_o - \Theta_\ell$ whichever is less

F $= \Theta'_f - \Theta_f$ or $\Theta'_f - \Theta_o$ whichever is greater (it can be negative)

K_f thermal conductivity of ice-bonded permafrost

K_t thermal conductivity of thawed sediments

α_f thermal diffusivity of ice-bonded permafrost

ρc volumetric heat capacity of ice-bonded permafrost

q^* steady upward geothermal flux (negative)
$= K_f (\Theta_\ell - \Theta'_f)/B$

X depth beneath sea bed

χ $= x - X$

X(t) Depth beneath sea bed to top of ice-bonded permafrost at time t

X'(t) Depth beneath sea bed to bottom of ice-bonded permafrost at time t

β $= X' - X$

L latent heat of freezing per unit volume of sediment

q_t heat flux downward <u>into</u> upper surface, X, of ice-bonded permafrost (positive)
$= K_s \frac{\varepsilon}{X}$

q_f heat flux downward <u>from</u> upper surface, X, of ice-bonded permafrost

q'_f heat flux upward <u>from</u> lower surface, X', of ice-bonded permafrost

q'_t heat flux upward <u>into</u> lower surface, X', of ice-bonded permafrost

$Q_f = \int_0^t q_t dt$

$Q'_f = \int_0^t q'_f dt$

Q_s, Q'_s the quasi steady-state parts of Q_f and Q'_f, respectively

Q, Q' the transient parts of Q_f and Q'_f, respectively

To obtain representative numerical results for the model of Figure 3, we shall estimate the parameters for the initial condition (t=0) and the thermal properties from observations on shore. Then with the values of X, Θ_f and Θ_o inferred from the measurements previously discussed (Table 1), we shall obtain relations for the duration of submergence t, and the vertical distribution of temperature and permafrost. The principal difficulty stems from the requirement to determine rate of movement of the upper and lower boundaries of the ice-bonded permafrost.

INITIAL CONDITIONS AND THERMAL PROPERTIES

Temperature measurements through permafrost at onshore installations near Prudhoe Bay suggest the following generalized values for the initial temperature distribution (see Figure 4 of Gold and Lachenbruch, 1973).

$$B \simeq 600 \text{ m} \tag{1a}$$

$$\Theta_f' \simeq -1°C \tag{1b}$$

$$\Theta_\ell \simeq -11°C \tag{1c}$$

$$\frac{G_t}{G_f} \simeq 1.8 \tag{1d}$$

Where G_t and G_f represent the thermal gradients immediately below and above the base of permafrost (x=B) respectively. We believe that this gradient discontinuity corresponds to a discontinuity in conductivity under steady thermal conditions. Hence

$$q_f' = q_t'$$

and consequently

$$\frac{K_f}{K_t} = \frac{G_t}{G_f} \tag{2}$$

For gas-free aggregates it is convenient to represent the thermal conductivity as the geometric mean value of the conductivities of the constituents (Sass and others, 1971). Thus if ϕ is the volume percent of water

or ice we have

$$K_t \approx K_w^{\phi} K_s^{1-\phi} \tag{3a}$$

$$K_f \approx K_i^{\phi} K_s^{1-\phi} \tag{3b}$$

where

$$K_w \approx 1.3 \text{ cal/cm sec } °C \tag{4a}$$

$$K_i \approx 5.4 \text{ cal/cm sec } °C \tag{4b}$$

are respectively the conductivities of water and ice, and K_s is the mean conductivity of the remaining solids.

Combining 1d, 2, 3, and 4 yields

$$\phi \sim 40\% \tag{5}$$

which is consistent with observations made near the sea bottom (Osterkamp and Harrison, 1976).

For siliceous sediments of the type common in the Prudhoe Bay area, we have found that K_s is typically about 10 cal/cm sec °C. Using this value with (4) and (5) in equations 3 yields

$$K_t \sim 4.4 \text{ cal/cm sec } °C \tag{6a}$$

$$K_f \sim 7.8 \text{ cal/cm sec } °C \tag{6b}$$

Taking the volumetric heat capacity (ρc) as 0.5 cal/cm^3 °C for solids and 1.0 cal/cm^3 °C for water we obtain for the thermal diffusivity

$$\alpha_t \sim 0.0063 \text{ cm}^2/\text{sec} \tag{7a}$$

$$\alpha_f \sim 0.016 \text{ cm}^2/\text{sec} \tag{7b}$$

The latent heat of freezing for water is about 80 cal/cm^3; and for sediments with $\phi \sim 40\%$, it is

$$L = 32 \text{ cal/cm}^3 \tag{8}$$

The steady geothermal flux q^* is obtained by combining 1a, [illegible] and 6b.

$$q^* = K_f \frac{\Theta_\ell - \Theta'_f}{B}$$

$$= -1.3 \times 10^{-6} \text{ cal/cm}^2\text{sec}$$

$$= -41 \text{ cal/cm}^2\text{yr} \tag{9}$$

We are using the convention that heat flux is negative for a positive temperature gradient; i.e., upflux is negative, downflux is positive.

CONDITIONS AT THE BOUNDARIES OF ICE-BONDED PERMAFROST

The upper boundary, X. If the mean sea bottom temperature Θ_o is greater than the freezing temperature Θ_f, then $\varepsilon > 0$ and thawing will proceed downward from the sea bed. Simultaneously, deposition of sediments will result in thickening of the thawed layer by the amount D(t) (see Figure 4). Therefore the heat balance at x=X is given by

$$\frac{dX}{dt} = \frac{q_t}{L} - \frac{q_f}{L} + \frac{dD}{dt} \tag{10}$$

For the large moisture contents under consideration and relatively small sedimentation rates, X will change slowly, and temperatures within the thawed layer can be considered in a quasi-steady state. We introduce $Q_f(t)$, the total amount of sensible heat supplied to the ice-bonded permafrost through its upper surface

$$Q_f(t) = \int_0^t q_f \, dt \tag{11}$$

and (10) can be written

$$\frac{dX}{dt} = \frac{K_s}{L} \frac{\varepsilon}{X} - \frac{1}{L} \dot{Q}_f + \dot{D} \tag{12}$$

where the dot denotes differentiation with respect to time.

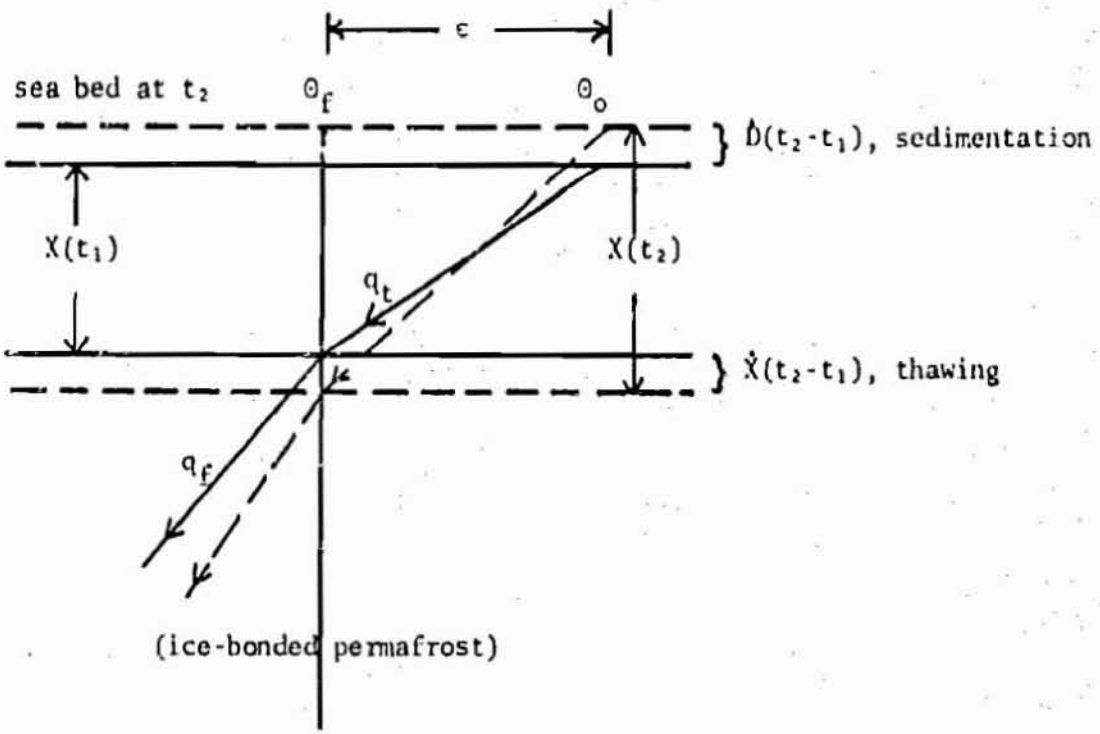

Figure 4. Simplified conditions in thawed layer to depth X beneath the sea bed at two successive times t_1 (solid lines) and t_2 (dashed lines) for case $\varepsilon > 0$. Θ_o and Θ_f assumed constant and quasi-steady conduction is assumed above X. Arrows on temperature curves represent heat fluxes q_t and q_f associated with gradients above and below X, respectively.

Equation 12 can be integrated simply if Q_f and D vary either as $t^{1/2}$ or t. The first case leads to

$$t = \frac{L}{2K_s}\frac{X^2}{\varepsilon}\left[1 - \frac{D}{X} + \frac{Q_f}{L}\frac{1}{X}\right] \tag{13}$$

and the second case yields

$$t = \frac{1}{p}\left[X - \frac{K_t\varepsilon}{Lp}\ln\left(1 + \frac{pL}{K_t\varepsilon}X\right)\right] \tag{14a}$$

$$\text{where } p = \dot{D} + \frac{\dot{Q}_f}{L}\ , \quad \text{a constant} \tag{14b}$$

In this report, we shall consider only the first case, equation 13, which gives the time t since submergence for a case in which both the sensible heat absorbed by permafrost and the sedimentation rate are very large initially and then diminish progressively. Qualitatively, this is correct for the heat; the behavior of sedimentation rate is unknown but at least (13) provides a first-order account of it. The factor preceding the bracket in (13) is the well known approximation that neglects sedimentation, and the more important effect of sensible heat absorbed by permafrost.

For the case $\varepsilon < 0$, there is, of course, no progressive thawing of the upper ice-bonded surface and $X = 0$.

The lower boundary, X'. The position of the lower boundary of ice-bonded permafrost, X' is determined by

$$L\frac{dX'}{dt} = q'_t - q'_f \tag{15a}$$

As the moisture content is large, X' will move slowly and we assume a quasi-steady state below the base of permafrost (i.e., in $x > X'$) and replace q'_t by q^*, the steady geothermal flux. Equation 15 can then be written

$$L\frac{dX'}{dt} = q^* - q'_f \tag{15b}$$

which yields on integration

$$B - X'(t) = -\left[\frac{q^*}{L}t - Q'_f(t)\right] \tag{16}$$

This is an expression for the thinning of ice-bonded permafrost from below after passage of time t since submergence. Unlike conditions at the upper surface, this thawing occurs irrespective of the sign of ε.

Our strategy is now as follows: In the next section we shall obtain expressions for Q_f and Q'_f. We can then apply our observations of X, ε, and D to estimate (from 13) the time of submergence t at any site. Introducing t and q^* in (16) will yield the position of the bottom of permafrost. Knowing the history of the positions of the phase boundaries

and the initial temperature distribution, we can then estimate the temperature distribution beneath any point on the sea bed.

THERMAL CONDITIONS WITHIN PERMAFROST AND THE EVALUATION OF EQUATIONS 13 AND 16

Conditions controlled primarily at the upper surface X. The rate at which heat enters the top (x=X) of ice-bonded permafrost consists of two parts; a quasi-steady part, $\dot{Q}_s$, resulting from the constant difference in temperature between its top X and bottom X', and a transient part, $\dot{Q}$, resulting from the depletion of its initial cold reserve (i.e., the heat needed to raise the temperature to melting). Hence

$$q_f = \dot{Q}_s + \dot{Q} \tag{17}$$

and (see Figures 3a, b)

$$\dot{Q}_s = -K_f \frac{F}{X'-X} \tag{18}$$

where $F = \Theta'_f - \Theta_f \quad \varepsilon > 0$

$$= \Theta'_f - \Theta_o \quad \varepsilon < 0$$

The transient part contributes heavily for early times (see e.g., curves t_1, Figure 3), but it becomes negligible (e.g., curves t_3, Figure 3) for later times. It will be shown (a posteriori) that for the ice-rich conditions at Prudhoe Bay, the transient decays before appreciable

permafrost thinning takes place. Hence, we can approximate the transient behavior by the temperature in a slab of constant thickness B with an initial linear temperature distribution, and with upper and lower surfaces maintained at constant temperature for $t > 0$.

For the sake of generality, we introduce the notation

$$\beta = X'(t) - X(t) \tag{19a}$$

$$\chi = x - X(t) \tag{19b}$$

but we shall ignore for the moment the time-dependence of X and X', and in the numerical calculations we shall generally approximate β by B, showing eventually that the approximation is probably of little consequence for the cases of interest.

We can write

$$\dot{Q} = K_f \left.\frac{\partial \Theta_i}{\partial \chi}\right|_{\chi=0} \tag{20}$$

where $\Theta_i(t,\chi;\beta)$ is the solution to

$$\frac{\partial^2 \Theta_i}{\partial \chi^2} = \frac{1}{\alpha_f} \frac{\partial \Theta_i}{\partial t} \quad , \quad 0 < \chi < \beta \tag{21}$$

with the conditions

$$\Theta_i = -E(1-\frac{\chi}{\beta}) \quad , \quad t = 0 \tag{22}$$

$$\Theta_i = 0, \ \chi=0 \text{ and } \chi=\beta \quad , \quad t > 0 \tag{23}$$

Here $$E = \Theta_f - \Theta_\ell \text{ for case } \varepsilon > 0 \tag{24}$$

$$E = \Theta_o - \Theta_\ell \text{ for case } \varepsilon < 0 \tag{25}$$

The solution (modified from Carslaw and Jaeger, 1959, p. 313, equation 10) is

$$\Theta_i(t,\chi;\beta) = \frac{2E}{\pi} \sum_{n=1}^{\infty} \frac{(-1)^n}{n} e^{\frac{-n^2\pi^2}{4}\frac{t}{\tau}} \sin[n\pi(1-\frac{\chi}{\beta})] \tag{26}$$

where the time constant τ is given by

$$\tau = \frac{\beta^2}{4\alpha_f} \tag{27a}$$

$$\approx 1800 \text{ yrs for Prudhoe Bay} \tag{27b}$$

where (27b) is obtained from (1a) and (7b), assuming $\beta \approx B$. Results from (26) are shown graphically in Figure 5. It is seen that the decay of Θ_i is almost complete (i.e., the sensible heat storage is negligible) for $t > \tau$. Hence it is necessary only that our approximation $\beta \approx B$ be valid for $t < \tau$.

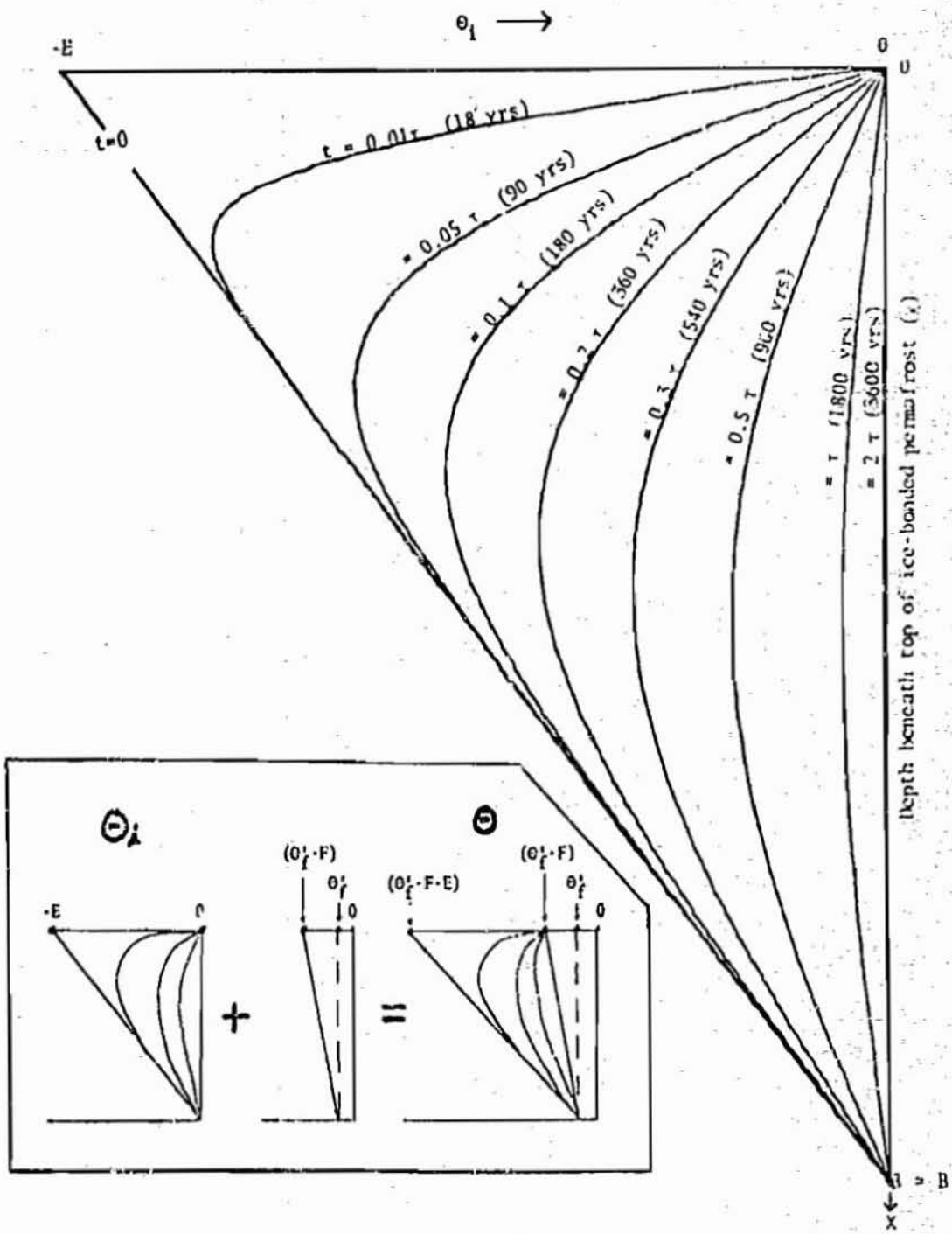

Figure 5. Transient temperature function Θ_i describing depletion of the cold reserve of ice-rich permafrost. Numbers on curves are times since inundation in dimensionless units (τ) and years for conditions at Prudhoe Bay. Inset shows scheme of temperature superposition.

Evaluating the derivative of (26) at $\chi=0$ yields an approximation to $\dot{Q}$.

$$\dot{Q} \simeq 2K_f \frac{E}{\beta} \sum_{n=1}^{\infty} e^{\frac{-n^2\pi^2}{4}\frac{t}{\tau}} \tag{28}$$

Integration of (28) yields Q(t), the total transient contribution after time t

$$Q(t) \equiv \int_0^t \dot{Q}\, dt$$

$$= \frac{4}{3} K_f \frac{E}{\beta} \tau \left[1 - \frac{6}{\pi^2} \sum_{1}^{\infty} \frac{1}{n^2} e^{\frac{-n^2\pi^2}{4}\frac{t}{\tau}}\right] \tag{29a}$$

$$= \frac{4}{3} K_f \frac{E}{\beta} \tau[1 - .05] \quad , \quad t=\tau \tag{29b}$$

$$\simeq \frac{4}{3} K_f \frac{E}{\beta} \tau \quad , \quad t > \tau \tag{29c}$$

Integration of (17) yields

$$Q_f(t) \equiv \int_0^t q_f\, dt$$

$$= Q(t) + \int_0^t \dot{Q}_s\, dt$$

$$\simeq \frac{K_f}{B} \left[\frac{4}{3} (E)\, \tau - (\Theta_f' - \Theta_f)t\right] \quad , \quad \varepsilon > 0 \quad , \quad t > \tau \tag{30}$$

Substituting the foregoing numerical values including Θ_f = -1.8°C, Θ'_f = -1°C in (30), we obtain the following dimensional relation for Prudhoe Bay

$$\frac{Q_f}{L'} \text{ (meters)} = 28 - 0.1 \times t \text{ (centuries)} \quad t > \tau \tag{31}$$

Introducing (31) in equation 13 along with observed values of marine sedimentation D and the other parameters, we obtain an estimate of the time since submergence (column 15, Table 1). The 28 meters contributed by the transient term in (30) is substantial, and the sensible heat it represents cannot be neglected. (The heat absorbed through the upper surface by the warming permafrost is equivalent to that required to melt 28 m of ice-bonded permafrost.) The second term in (31) represents the quasi-steady effect and it is sensitive to the choice of Θ_f and Θ'_f, the latter in particular is rather arbitrary. In Table 1, column 8, the simpler approximation neglecting sedimentation and sensible heat is compared with the adjusted values, Table 1, column 15, given by equation 13, still a crude approximation. In general, the combined effect of sedimentation and heat storage increases the estimate of t by about 45%.

It is seen from Table 1, column 7, that (excluding PB-1, to be discussed) the greatest thawing from the surface, X - D, is about 40 m. It occurs at hole 3370 where the time t (column 15) is substantially greater than τ. But 40 m is only 7% B, and at $t=\tau$, X - D would be

appreciably less. Therefore thawing from the top of ice-bonded permafrost does not seriously jeopardize our approximation

$$\beta(\tau) \approx B$$

More general conditions for the validity of the approximation will be considered elsewhere.

Returning now to the case $\varepsilon < 0$ we should like to determine the temperature gradient $\left.\frac{\partial \Theta}{\partial X}\right|_0$ near the sea bed in ice-bonded permafrost as a function of time to compare with the observed value at hole #190. From (17), (18), and (28) it is given approximately by

$$-\left.\frac{\partial \Theta}{\partial X}\right|_0 = \frac{q_f}{K_f}$$

$$\approx \frac{1}{B}\left\{\Theta_f' - \Theta_o + 2(\Theta_o - \Theta_\ell) \sum_{n=1}^{\infty} e^{\frac{-n^2\pi^2}{4}\frac{t}{\tau}}\right\} \qquad (32)$$

or

$$2 \sum_{n=1}^{\infty} e^{\frac{-n^2\pi^2}{4}\frac{t}{\tau}} \approx \frac{1}{\Theta_o - \Theta_\ell}\left\{-B \left.\frac{\partial \Theta}{\partial X}\right|_0 - (\Theta_f' - \Theta_o)\right\} \qquad (33)$$

From Figure 2, we obtain $\left.\frac{\partial \Theta}{\partial X}\right|_0 \approx -38°C/km$, and $\Theta_o = -3.5°C$ for hole 190.

Introducing the other parameters in (33) yields

$$B \left.\frac{\partial \Theta}{\partial x}\right|_0 = -22.8°C$$

$$\Theta'_f - \Theta_o = 2.5°C$$

$$\Theta_o - \Theta_\ell = 7.5°C$$

and (33) yields

$$2 \sum_{n=1}^{\infty} e^{\frac{-n^2\pi^2}{4}\frac{t}{\tau}} = 2.70 \qquad (34)$$

This relation is satisfied by

$$\frac{t}{\tau} \simeq .08 \qquad (35a)$$

$$t \simeq 145 \text{ yrs} \qquad (35b)$$

This value is consistent with an estimate by Harrison (oral communication) made with another method (it will be discussed further below).

Melting from the lower surface X'. Following the procedure used for the upper surface, we break q'_f into its transient and steady parts.

$$q'_f = \dot{Q}'_s + \dot{Q}' \tag{36}$$

where

$$\dot{Q}'_s = \dot{Q}_s = -K_f \frac{F}{X'-X} \tag{37}$$

We shall also use the notation

$$Q'_f = \int_0^t q'_f \tag{38}$$

$$= Q'_s + Q'$$

The heat balance at the lower surface X' of ice-rich bonded permafrost is given by (15b), integration of which yields

$$-L \int_B^{X'} dX' = \int_0^t [q'_f - q^*] \, dt \tag{39}$$

$$B-X' = \frac{1}{L} \left(Q'(t) - \int_0^t K_f \frac{F}{B} \, dt - q^* \, t\right) \tag{40}$$

It has been shown that $Q'(t)$ will not increase significantly after t exceeds τ, i.e., by time τ the sensible cold reserve has been depleted. The total amount of heat input from top and bottom required to achieve this depleted condition is

$$Q_f(\tau) - Q_f'(\tau) \simeq \frac{1}{2} \rho c \, B \, E \tag{41a}$$

$$\simeq 2 \, K_f \frac{E}{B} \tau \tag{41b}$$

where (41b) follows from (27a)

Substituting (29c) yields

$$-Q_f'(\tau) \simeq \frac{2}{3} K_f \frac{E}{B} \tau \tag{42}$$

Comparing (41b) and (42) we see that one-third of the sensible heat required to warm the permafrost enters through to bottom surface.

Integrating (40) and using (42) we obtain for $t = \tau$

$$B - X'(\tau) \simeq \frac{1}{L} \left\{ \frac{-2}{3} K_f \frac{E}{B} \tau - K_f \frac{F}{B} \tau - q^* \tau \right\}$$

but $$q^* = -K_f \frac{E+F}{B}$$

and hence

$$B - X'(\tau) \approx \frac{1}{3L} K_f \frac{E}{B} \tau \qquad (43)$$

From (43) we can calculate the thinning of permafrost from the bottom during the first 1800 yrs ($t=\tau$) after submergence for the four offshore sites where $E \approx 9.2°C$ and for hole 190 where $E \approx 7.5°$

$$B - X'(\tau) = 7 \text{ m} \quad , \quad t = 1800 \text{ yrs}, \; E = 9.2°C \qquad (44a)$$

$$= 5.7 \text{ m} \quad , \qquad E = 7.5°C \qquad (44b)$$

As this is only about 1% of B, thinning from the bottom will not jeopardize our approximation

$$\beta(\tau) \approx B$$

For larger values of time ($t > \tau$), the first term in the braces, equation 40, is constant. Using (43), the subsequent thawing can be expressed

$$B - X'(t) \approx \frac{K_f E}{3LB} \tau - \frac{1}{L} \left(q^*(t-\tau) - \int_\tau^t K_f \frac{E}{\beta} dt\right) \qquad (45a)$$

$$\approx \frac{K_f E}{3LB} \tau + \frac{1}{L} \left(K_f \frac{E+F}{B} (t-\tau) - \int_\tau^t K_f \frac{F}{\beta} dt\right) , \quad t > \tau \qquad (45b)$$

Thus if F is small relative to E as is generally true in the case $\varepsilon > 0$, the constant degradation for $t > \tau$ caused by the geothermal flux will adequately describe all but the final stages of permafrost melting ($\beta << B$).

We can describe the melting of the bottom of permafrost for $t > \tau$, taking account of the time-dependence of β in (45). For the small values of ε and large values of L of interest, it is seen from (13) and (16) that most of the permafrost thinning will take place from below for larger values of time. Retaining only X' in the denominator of the right side of (37) and observing that $\dot{Q}' \approx 0$ for $t > \tau$ we obtain

$$q_f' \approx -K_f \frac{F}{X'} \quad , \quad t > \tau \tag{46}$$

The heat balance (15b) can then be written

$$L \frac{dX'}{dt} = -|q^*| + K_f \frac{F}{X'} \quad , \quad t > \tau \tag{47}$$

As q^* is negative by our convention, we insert the absolute value to clarify the physical meaning of (47). It follows that

$$\int_\tau^t dt = \int_{X'(\tau)}^{X'(t)} \frac{X'}{\frac{K_f F}{L} - \frac{|q^*|}{L} X'} dX'$$

or

$$t - \tau = \frac{L}{|q^*|} [X'(\tau) - X'(t)] \{1 + \frac{H}{X'(\tau) - X'(\tau)} \ln [\frac{X'(\tau) - H}{X'(t) - H}]\} \quad (48a)$$

$$\simeq \frac{L}{|q^*|} [X'(\tau) - X'(t)] \quad , \quad H \simeq 0 \quad (48b)$$

$$\frac{L}{|q^*|} \simeq 0.78 \text{ centuries/meter, Prudhoe Bay} \quad (48c)$$

where (48c) follows from (8) and (9). In (48) H is a characteristic length defined by

$$H = \frac{FK_f}{|q^*|} \quad (49a)$$

$$= \frac{F}{E+F} B \quad (49b)$$

$$= \frac{\Theta'_f - \Theta_f}{\Theta'_f - \Theta_\ell} B \quad \text{for } \varepsilon > 0 \quad (49c)$$

$$= \frac{\Theta'_f - \Theta_o}{\Theta'_f - \Theta_\ell} B \quad \text{for } \varepsilon < 0 \quad (49d)$$

Equation 48a gives the time past $t=\tau$ required for the bottom of permafrost to rise to $X'(t)$ (from $X'(\tau)$ given by equation 43). The factor preceding the braces is the simple thawing by geothermal flux (48b). If the melting temperature is the same at the top and bottom of permafrost,

then F=0, and the quantity in braces is unity; the ice-bonded permafrost will eventually all disappear, degrading at a near-constant rate (48b and c). If $F > 0$ the degradation will proceed at a diminishing rate and a steady state will occur when $X'/B = F/(E+F)$. If $F < 0$, the second term in braces becomes negative and the quasi-steady flux across the ice-bonded permafrost accelerates thawing. (The final stages may, of course, be complicated by variations of Θ_f', and for $\varepsilon > 0$, by behavior of the upper surface.)

For the four offshore holes where $F = 0.8°$, $E = 9.2°$, the expression in braces can generally be neglected, and thawing can be computed at the rate L/q^* (or 1.28 m/century, see equation 48c) for times of interest at Prudhoe Bay. For example, for X' to reduce to 500 m from 593 m, neglecting the braces gives $(t-\tau) = 7{,}250$ yrs and including them gives 8,030 yrs. The total time, obtained by adding τ (during which time the first 7 m thawed), is 9,050 yrs neglecting braces or 9,830 accounting for them. If the model is approximately correct, it is likely that ice-bonded permafrost extends to depths on the order of 500 m beneath the observation sites at Prudhoe Bay today.

Temperature profiles. A summary expression for the approximate temperature $\Theta(x,t)$ above, in, and beneath ice-rich bonded permafrost according to the present model is

Case I $\quad \varepsilon \equiv \Theta_o - \Theta_f > 0$

$$\Theta \approx \Theta_o - \frac{\varepsilon}{X} x \quad , \quad 0 < x < X \tag{50a}$$

$$\approx \Theta_f + \Theta_i(t,\chi;\beta) + \frac{F}{\beta}(x-X(t)) \quad , \quad X < x < X' \tag{50b}$$

$$\approx \Theta'_f - \frac{q^*}{K_t}(x-X') \quad , \quad x > X' \tag{50c}$$

Case II $\quad \varepsilon \equiv \Theta_o - \Theta_f < 0$

$$\Theta \approx \Theta_o + \Theta_i(t,\chi;\beta) + \frac{F}{\beta} x \quad , \quad 0 < x < X' \tag{51a}$$

$$\approx \Theta'_f - \frac{q^*}{K_t}(x-X') \quad , \quad x > X' \tag{51b}$$

The quantities X and X' are functions of t given by equations 13 and 16, respectively, and $\Theta_i(t,\chi;\beta)$ is given by equation 26. For approximations under ice-rich conditions and small ε such as those at Prudhoe Bay we can generally replace β by B in Θ_i without serious error For $t < \tau \approx 1800$ yrs at Prudhoe Bay, the temperature profiles will resemble curves t_1 or t_2 of Figure 3a for case I, and Figure 3b for case

II. For $t > \tau$, Θ_i is small and the profiles will resemble curves t_3 of Figure 3a for case I, and Figure 3b for case II. Parameters for the profiles beneath each study site can be obtained from Table 1 and relations in the text. Numerical details of the results should not be taken too seriously, however, until more data are acquired to confirm the assumptions or refine the analysis.

SUMMARY AND DISCUSSION

We have presented a highly simplified analysis of thermal conditions near the shore at Prudhoe Bay. Although it cannot be "right" in detail, the exercise exposes some logical implications of the fragmentary observations presently available, it indicates the sensitivity of these implications to several of the parameters upon which the solution depends, and it serves to focus attention on the types of observations needed for a more confident analysis. The principal assumptions are:

1) Thawed sediments at the sea bed are saturated with normal sea water

2) Salinity of the ice-bonded permafrost is negligible

3) Prior to the last inundation, the thermal regime was in a steady state and similar to the regime observed beneath the adjacent land today

4) The sediments are generally siliceous and have a large porosity

5) The thermal conductivity of the ice-bonded and thawed material are each relatively uniform

6) The mean sea-bottom temperature inferred from present-day observations at each site is the value that has obtained since inundation

7) Horizontal heat transport is negligible relative to vertical transport.

A rather indirect justification for the first assumption has been presented in the section "Temperature Measurements"; it can easily be

confirmed by deeper drilling. Some justification for assumptions 2, 4, and 5 is provided by limited information on materials and temperatures from boreholes on and off shore. The validity of assumption 3 depends upon interpretations of shoreline chronology; the assumption is probably consistent with existing evidence at the sites under study (see Hopkins and others, 1977). Assumption 6 is arbitrary and justified largely by its simplicity and our present lack of information; more rational refinements are possible but probably unwarranted at this stage. The seventh assumption will generally be violated at sites near shore.

The analysis yields the following results:

1) It underscores the importance of distinguishing between two cases:

a) $\varepsilon > 0$, and

b) $\varepsilon < 0$

where $\varepsilon = \Theta_o - \Theta_f$ and Θ_o is the mean sea bed temperature and Θ_f is the temperature of the upper boundary of ice-bonded permafrost (see Figure 3). In the first case ($\varepsilon > 0$), permafrost thaws downward progressively from the sea bed and eventually disappears. In the second case ($\varepsilon < 0$), permafrost persists near the sea bed, even in the steady state. The second case is expected in a near-shore band where sea-ice freezes to the bottom seasonally, but it is also possible at offshore locations. Θ_o depends on the seasonal regime of the sea water and Θ_f depends upon salt transport mechanisms in the sea bed; small changes in the relative values of Θ_o and Θ_f can change the sign of ε and convert one regime to

the other. Several aspects of this problem have been discussed in detail by Harrison and Osterkamp (1976) and Osterkamp (1975).

2) When the cold permafrost is inundated by the sea, it absorbs heat from the relatively warm sea bed above and from geothermal flux rising from below. After an initial period, the duration of which is easily calculated, temperatures in the ice-bonded permafrost become nearly uniform at the value determined by the melting temperatures of its upper and lower surfaces. For conditions at Prudhoe Bay the time required to reach this near-isothermal condition is about 1800 years; for submergence times less than this, appreciable negative thermal gradients are expected beneath the top of ice-bonded permafrost.

3) A substantial amount of the heat conducted downward through the sea bed is consumed in warming the permafrost to its melting temperature (not melting it) in the initial phases. For conditions at Prudhoe Bay, the total amount of this heat is equivalent to that required to melt 28 m of ice-bonded permafrost. This heat requirement, neglected in simpler models, can have a substantial effect on the estimate of time of inundation calculated from the observed depth of thawing at the sea bed. For the present data it increases the time by 50%-80% (Table 1, column 13).

4) One-third of the heat required to deplete the initial sub-freezing cold reserve of permafrost is supplied by geothermal flux entering through the lower boundary. Thus, for conditions at Prudhoe Bay the lower surface of permafrost rises only about 7 m during the

first 1800 years, and thereafter it rises at the near-constant rate of about 1 1/4 m/century.

5) The rate of thawing of the upper surface of ice-bonded permafrost diminishes progressively with time because the thickness of the insulating thawed layer increases. According to the model, the present rate of thawing of the upper surface of ice-bonded permafrost is about 1 cm/yr at [illegible], 1/2 cm/yr at PB-3, and 1/3 cm/yr at PB-2. Hence at present, permafrost is degrading faster at its lower surface (1 1/4 cm/yr, see 4) above) than at its upper surface at all sites, and the disparity will increase with time. According to our interpretation of the thermal data, the thawed layer at the sea bed is thinnest at PB-2 (column 7, Table 1), the site that is farthest from shore, and hence the one that has been submerged the longest. The analysis resolves this paradox because the sea bed at PB-2 is colder and it thaws more slowly, as indicated by the rates just cited (see also Table 1, columns 4 and 6). These conclusions are sensitive to assumptions 6 and 7 which could be seriously violated at PB-2, for example, by migration of Reindeer Island. Uncertainties of this sort can easily be resolved with additional drilling for thermal observations.

6) The rate of sedimentation plays an important role in the heat transfer between the sea bottom and the upper surface of ice-bonded permafrost. The thickness of the thawed layer that insulates permafrost is the combined effect of thawing and sedimentation. Failure to account

for sedimentation can lead to substantial errors in attempts to estimate the period of inundation from observations of temperature and thickness of the thawed layer beneath the sea bed. A very crude mathematical account of sedimentation leads to adjustments of the inundation time by as much as 40% at the Prudhoe Bay sites; more realistic accounts will probably have larger effects.

With all of its shortcomings, the analytical model was applied formally to observations at holes #190, #3370, PB-3, and PB-2. The calculated effective time of inundation is shown in Figure 6 as a function of distance from the present shoreline (see also Table 1, column 15). Taken at face value, the results suggest a period of rapid transgression (at the rate of 10 m/yr) terminating some 4000 years ago at a point presently perhaps 4 or 5 km from shore. Thereafter, they suggest a slow transgression at the rate of 1 m/yr up to the present shoreline position. The latter rate is consistent with geomorphic estimates of thermal erosion of the present shoreline (see Hopkins and others, 1977); the former would suggest a rapid rise of sea level in the past. However, these numerical results should not be taken too seriously; it is easy to think of uncertainties in the assumptions that could change the results substantially. It is probably fortuitous that the rate of transgression, 10 m/yr, from PB-2 to PB-3 (Figure 6) is the same as the value determined by Hopkins (written communication) from sea level curves; a completely independent source of information. The absolute values of his times of inundation are generally larger than

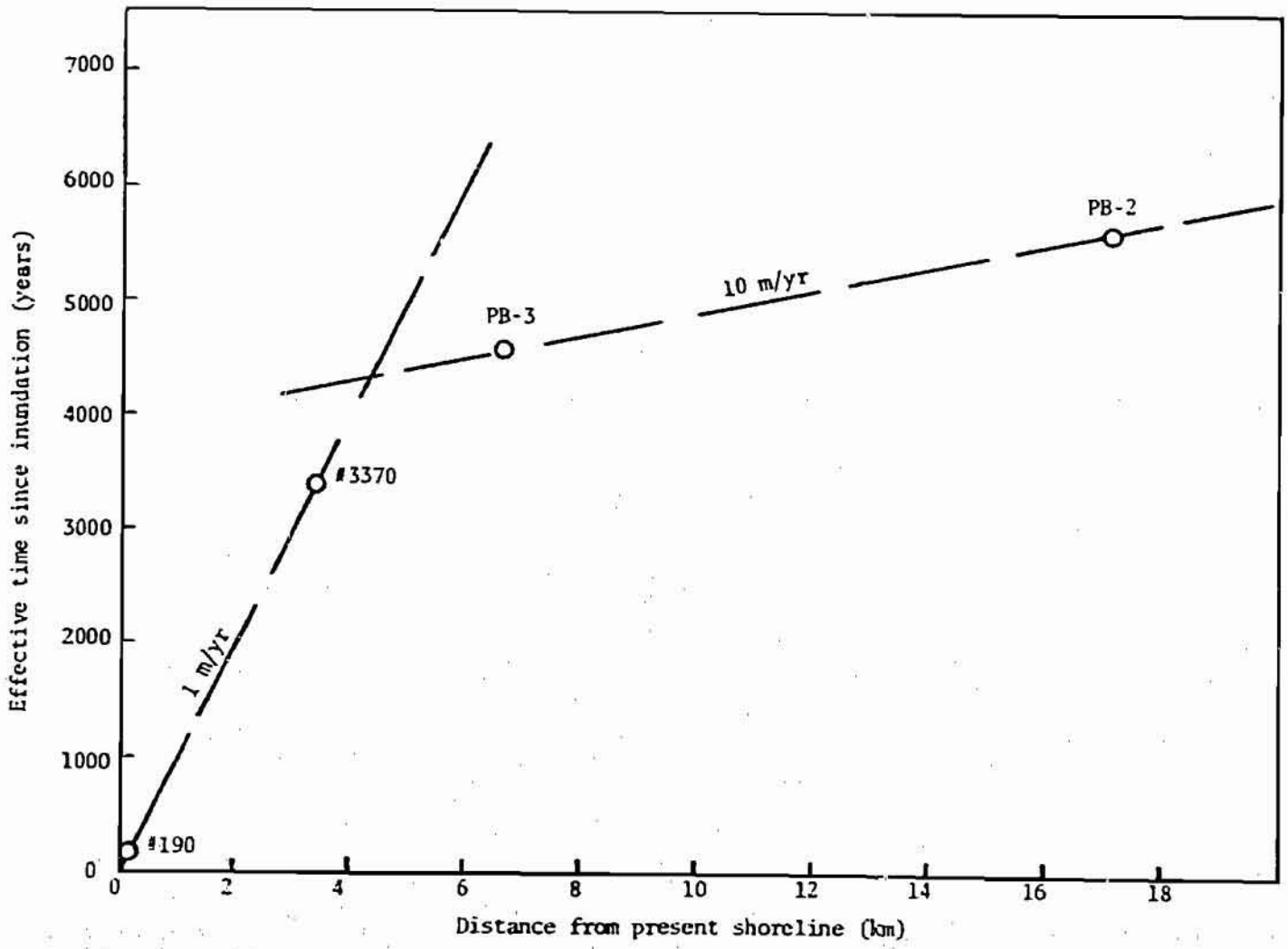

Figure 6. Effective time since inundation, t, determined from formal application of equation 13 for the three offshore holes and equation 35b for #190. Slopes of dashed lines suggest rate of shoreline transgression.

ours by a factor of about 2, and consequently his estimate of the transgression rate for the most recent phase is about half of ours (about 1/2 m/yr). (One other curious, and perhaps no less fortuitous result of our calculation is that hole 3370 which is 3370 m from shore has a calculated inundation time of 3370 years.)

As the three offshore holes all have inundation times substantially greater than the 1800 years required to deplete the cold reserve, the analysis indicates that the temperature profiles beneath these holes are described by the curve labeled t_3 in Figure 3a. That is the ice-bonded permafrost is nearly isothermal and near its melting temperature. The temperature and depth parameters (Θ_o, Θ_f, X, X') for the curves at each site are given in Table 1. Note that the base of permafrost has risen only a few tens of meters (column 16). Thus the model suggests that near isothermal ice-rich permafrost (at temperatures close to melting) extends to depths of 500 m or so beneath the four offshore holes.

Temperatures beneath hole 190 would follow a curve like t_1, Figure 3b. According to the model, the actual position of the transient part of this curve is about midway between curves labeled $\tau = 0.05$ and $\tau = 0.1$, Figure 5. The curve parameters Θ_o, Θ_f, X and X' are given in Table 1; Θ_ℓ and Θ_f' can reasonably be assumed to be -11°C and -1°C, respectively. For a refined analysis at this site, departures from assumption 7 should be examined.

The hole PB-1 lies within Prudhoe Bay proper, a bathymetric basin (see Figure 1). PB-1 and hole 3370 are both about 3 km from shore, and

their sea-bed temperatures measured to depths of 20+ m are comparable (Figure 2). However, the thermal gradient is anomalously low at PB-1. A formal extrapolation to the -1.8° isotherm yields a thaw depth of 80± m, and a formal calculation of the duration of submergence yields 13000+ years for PB-1 (Table 1). There are two simple ways of explaining this anomaly:

1) The sediments beneath PB-1 contain water of low salinity and consequently the top of ice-bonded permafrost lies well above the -1.8°C isotherm, i.e., Θ_f is relatively high.

2) The sediments at PB-1 were "pre-heated" beneath a large thaw lake whose shoreline eventually was breached by the sea to form Prudhoe Bay proper. Mean annual bottom temperatures of large thaw lakes on the coastal plain generally vary from about 0°C to about +1.5°C depending upon whether or not they are brackish; where the lakes are less than 2 m deep their temperatures can be lower (Lachenbruch and others, 1962). Thus the negative temperature gradient at PB-1 tends to support the first explanation although it does not preclude the second. A recent radiocarbon date suggests that marine conditions commenced at PB-1 only 600 years ago (David Hopkins, written communication). As this allows little time for thawing, it supports the ancestral lake explanation. The problem can be resolved by drilling to 100 m in Prudhoe Bay; the resolution bears upon the question of whether or not ice-rich permafrost exists beneath Prudhoe Bay proper.

APPENDIX

Temperature Measurements in Holes PB-1, PB-2, and PB-3

Hole PB-1

Date: April 12, 1976 Depth of ice and water: 2.68 m

Depth (m) (below sea bed)	Temperature (°C)
5.85	-1.249
6.46	-0.972
7.99	-0.965
9.51	-0.967
11.03	-0.973
12.56	-0.993
14.08	-0.998
15.61	-1.014
17.13	-0.977
18.65	-1.026
20.18	-1.062
21.58	-1.065

Hole PB-1

Date: April 14, 1976 Depth of ice and water: 2.68 m

Depth (m) (below sea bed)	Temperature (°C)
5.24	-1.272
5.85	-1.089
6.46	-1.076
7.07	-1.070
7.68	-1.067
8.29	-1.066
8.90	-1.070
9.51	-1.073
10.12	-1.077
10.73	-1.081
11.34	-1.089
11.95	-1.098
12.56	-1.105
13.17	-1.108
13.78	-1.107
14.39	-1.107
15.00	-1.111
15.61	-1.112
16.22	-1.107
16.82	-1.096
17.43	-1.092
18.04	-1.105
18.65	-1.125
19.26	-1.145
20.18	-1.166
21.58	-1.357

Hole PB-1

Date: April 23, 1976 Depth of ice and water: 2.68 m

Depth (m) (below sea bed)	Temperature (°C)
5.24	-1.326
5.85	-1.151
6.46	-1.135
7.07	-1.129
7.68	-1.126
8.29	-1.124
8.90	-1.125
9.51	-1.124
10.12	-1.121
10.73	-1.125
11.34	-1.127
11.95	-1.127
12.56	-1.133
13.17	-1.136
13.78	-1.140
14.39	-1.140
15.00	-1.141
15.61	-1.143
16.22	-1.146
16.82	-1.160
17.43	-1.168
18.04	-1.172
18.65	-1.179
19.26	-1.181
19.87	-1.177
20.48	-1.186
21.09	-1.209
21.64	-1.215

Hole PB-1

Date: May 3, 1976 Depth of ice and water: 2.68 m

Depth (m) (below sea bed)	Temperature (°C)
5.85	-1.184
6.46	-1.162
7.07	-1.152
7.68	-1.141
8.29	-1.144
8.90	-1.142
9.51	-1.145
10.12	-1.145
10.73	-1.149
11.34	-1.153
11.95	-1.157
12.55	-1.162
13.17	-1.166
13.78	-1.170
14.39	-1.172
15.00	-1.177
15.61	-1.180
16.22	-1.181
16.82	-1.184
17.43	-1.190
18.04	-1.193
18.65	-1.199
19.26	-1.202
19.87	-1.206
20.48	-1.213
21.09	-1.218
21.55	-1.225

Hole PB-1

Date: June 8, 1976 Depth of ice and water: 2.68 m

Depth (m) (below sea bed)	Temperature (°C)
6.10	-1.301
6.71	-1.236
7.32	-1.216
7.92	-1.202
8.53	-1.193
9.14	-1.186
9.75	-1.182
10.36	-1.180
10.97	-1.180
12.19	-1.182
13.72	-1.188
15.24	-1.197
16.76	-1.206
18.29	-1.216
19.81	-1.227
21.34	-1.239
21.55	-1.243

Hole PB-2

Date: April 21, 1976

Depth of ice and water: 11.65 m

Depth (m) (below sea bed)	Temperature (°C)
0.55	-1.559
1.16	-1.512
1.77	-1.492
2.38	-1.479
2.99	-1.466
3.60	-1.458
4.21	-1.452
4.82	-1.452
5.43	-1.453
6.04	-1.455
6.64	-1.458
7.25	-1.463
7.86	-1.466
8.47	-1.475
9.08	-1.485
9.69	-1.532
10.30	-1.587
10.91	-1.607
11.52	-1.608
12.13	-1.603
12.74	-1.610
13.35	-1.614
13.96	-1.616
14.57	-1.614
15.18	-1.616
15.79	-1.626
16.40	-1.628
17.01	-1.631
17.62	-1.631
18.23	-1.631
18.84	-1.628
19.45	-1.625
20.06	-1.619
20.67	-1.606
21.28	-1.591
21.88	-1.580
22.49	-1.576
23.10	-1.584
23.71	-1.603
24.32	-1.652
24.93	-1.671
25.54	-1.684
26.15	-1.701
26.76	-1.711
27.37	-1.720
27.98	-1.727
28.59	-1.743
29.20	-1.755
29.38	-1.751

Hole PB-2

Date: April 26, 1970

Depth of ice and water: 11.65 m

Depth (m) (below sea bed)	Temperature (°C)
0.24	-1.679
0.55	-1.660
0.85	-1.658
1.16	-1.616
1.77	-1.588
2.38	-1.581
2.99	-1.551
3.60	-1.528
4.21	-1.515
4.81	-1.510
5.42	-1.514
6.03	-1.521
6.64	-1.532
7.25	-1.545
7.86	-1.561
8.47	-1.576
9.08	-1.599
9.69	-1.614
10.30	-1.623
10.91	-1.633
11.52	-1.639
12.13	-1.633
12.74	-1.638
13.35	-1.638
13.96	-1.643
14.57	-1.642
15.18	-1.654
15.79	-1.664
16.40	-1.667
17.01	-1.667
17.62	-1.668
18.23	-1.668
18.84	-1.671
19.45	-1.665
20.05	-1.687
20.66	-1.689
21.27	-1.686
21.88	-1.683
22.49	-1.684
23.10	-1.690
23.71	-1.696
24.32	-1.686
24.93	-1.685
25.54	-1.717
26.15	-1.751
26.76	-1.767
27.37	-1.774
27.98	-1.780
28.59	-1.787
29.20	-1.795
29.23	-1.794

Hole PB-2

Date: M / 6, 1976

Depth of ice and water: 11.65 m

Depth (m) (below sea bed)	Temperature (°C)
0.24	-1.688
0.55	-1.683
0.85	-1.674
1.16	-1.665
1.46	-1.651
1.77	-1.641
2.07	-1.630
2.38	-1.616
2.68	-1.605
2.99	-1.589
3.29	-1.576
3.60	-1.567
3.90	-1.560
4.21	-1.557
4.51	-1.554
4.81	-1.553
5.12	-1.554
5.42	-1.555
5.73	-1.558
6.03	-1.362
6.34	-1.566
6.64	-1.571
6.95	-1.575
7.25	-1.579
7.86	-1.592
8.47	-1.606
9.08	-1.621
9.69	-1.633
10.30	-1.639
10.91	-1.644
11.52	-1.648
12.13	-1.648
12.74	-1.652
13.35	-1.656
13.96	-1.659
14.57	-1.665
15.18	-1.673
15.79	-1.680
16.40	-1.686
17.01	-1.690
17.62	-1.692
18.23	-1.695
18.84	-1.698
19.45	-1.697
20.05	-1.707
20.66	-1.715
21.27	-1.720
21.88	-1.723
22.49	-1.725
23.10	-1.727
23.71	-1.725
24.32	-1.711
24.93	-1.705
25.54	-1.735
26.15	-1.761
26.76	-1.776
27.37	-1.784
27.98	-1.791
28.59	-1.797
29.20	-1.802
29.23	-1.802

Hole PB-2

Date: June 8, 1976

Depth of ice and water: 11.65 m

Depth (m) (below sea bed)	Temperature (°C)
0.15	-1.659
0.76	-1.648
1.37	-1.630
1.98	-1.615
2.59	-1.607
3.20	-1.599
3.81	-1.597
4.42	-1.597
5.02	-1.599
5.64	-1.604
6.25	-1.609
6.86	-1.618
7.48	-1.627
8.08	-1.636
8.69	-1.644
9.30	-1.648
9.91	-1.652
10.51	-1.656
11.12	-1.660
11.73	-1.664
12.34	-1.668
12.95	-1.671
13.56	-1.675
14.17	-1.682
14.78	-1.689
15.39	-1.697
16.00	-1.705
16.61	-1.711
17.22	-1.714
17.83	-1.717
18.44	-1.722
19.05	-1.726
19.66	-1.732
20.27	-1.736
20.88	-1.738
21.49	-1.738
22.10	-1.736
22.71	-1.732
23.32	-1.735
23.93	-1.741
24.54	-1.758
25.15	-1.770
25.75	-1.780
26.36	-1.789
26.97	-1.795
27.58	-1.800
28.10	-1.805

Hole PB-3

Date: May 1, 1976

Depth of ice and water: 5.84 m

Depth (m) (below sea bed)	Temperature (°C)
0.25	-1.502
0.86	-1.401
1.47	-1.345
2.08	-1.314
2.69	-1.295
3.30	-1.285
3.91	-1.282
4.52	-1.280
5.13	-1.278
5.74	-1.273
6.35	-1.273
6.96	-1.276
7.57	-1.287
8.18	-1.299
8.79	-1.312
9.40	-1.327
10.00	-1.342
10.62	-1.350
11.22	-1.358
11.83	-1.366
12.44	-1.373
13.05	-1.384
13.66	-1.395
14.27	-1.401
14.88	-1.404
15.49	-1.405
16.10	-1.410
16.71	-1.402
17.32	-1.407
17.93	-1.432
18.54	-1.452
19.15	-1.450
19.76	-1.449
20.37	-1.451
20.98	-1.454
21.59	-1.458
22.20	-1.465
22.81	-1.473
23.42	-1.487
24.03	-1.510
24.64	-1.528
25.25	-1.538
25.86	-1.541
26.46	-1.545
27.07	-1.549
27.68	-1.549
28.29	-1.545
28.90	-1.543
29.51	-1.547
30.12	-1.558
30.73	-1.571
31.34	-1.580
31.95	-1.592
32.56	-1.592
33.17	-1.576
33.78	-1.570
34.39	-1.585
35.00	-1.603
35.61	-1.601
36.22	-1.590
36.83	-1.575
37.44	-1.574
38.05	-1.579
38.66	-1.592
39.27	-1.588
39.87	-1.483
40.15	-1.374

Hole PB-3

Date: May 3, 1976

Depth of ice and water: 5.84 m

Depth (m) (below sea bed)	Temperature (°C)
0.25	-1.613
0.86	-1.491
1.47	-1.437
2.08	-1.442
2.69	-1.406
3.30	-1.375
3.91	-1.355
4.52	-1.341
5.13	-1.338
5.74	-1.337
6.35	-1.336
6.96	-1.337
7.57	-1.339
8.18	-1.345
8.79	-1.357
9.40	-1.365
10.01	-1.375
10.62	-1.383
11.22	-1.391
11.83	-1.399
12.44	-1.408
13.05	-1.418
13.66	-1.432
14.27	-1.441
14.88	-1.447
15.49	-1.450
16.10	-1.454
16.71	-1.453
17.32	-1.449
17.93	-1.470
18.54	-1.497
19.15	-1.502
19.76	-1.500
20.37	-1.500
20.98	-1.503
21.59	-1.506
22.20	-1.511
22.81	-1.518
23.42	-1.527
24.03	-1.547
24.64	-1.573
25.25	-1.583
25.86	-1.590
26.46	-1.597
27.07	-1.601
27.68	-1.602
28.29	-1.601
28.90	-1.597
29.51	-1.605
30.12	-1.623
30.73	-1.642
31.34	-1.652
31.95	-1.654
32.56	-1.652
33.17	-1.654
33.78	-1.657
34.39	-1.663
35.00	-1.677
35.61	-1.686
36.22	-1.690
36.83	-1.686
37.44	-1.684
38.05	-1.705
38.66	-1.709
39.27	-1.692
39.88	-1.654
40.18	-1.620
40.39	-1.599

Hole PB-3

Date: May 6, 1976

Depth of ice and water: 5.84 m

Depth (m) (below sea bed)	Temperature (°C)
0.25	-1.639
0.56	-1.598
0.86	-1.534
1.17	-1.474
1.47	-1.471
1.78	-1.473
2.08	-1.470
2.69	-1.443
3.30	-1.420
3.91	-1.404
4.52	-1.386
5.13	-1.366
5.74	-1.360
6.35	-1.360
6.96	-1.361
7.57	-1.364
8.18	-1.372
8.79	-1.380
9.40	-1.389
10.01	-1.398
10.62	-1.406
11.22	-1.415
11.83	-1.424
12.44	-1.434
13.05	-1.445
13.66	-1.456
14.27	-1.464
14.88	-1.469
15.49	-1.474
16.10	-1.478
16.71	-1.479
17.32	-1.484
17.93	-1.502
18.54	-1.521
19.15	-1.526
19.76	-1.528
20.37	-1.530
20.98	-1.534
21.59	-1.539
22.20	-1.544
22.81	-1.550
23.42	-1.560
24.03	-1.583
24.64	-1.597
25.25	-1.608
25.86	-1.618
26.46	-1.625
27.07	-1.629
27.68	-1.631
28.29	-1.633
28.90	-1.635
29.51	-1.643
30.12	-1.658
30.73	-1.673
31.34	-1.681
31.95	-1.686
32.56	-1.690
33.17	-1.697
33.78	-1.705
34.39	-1.715
35.00	-1.726
35.61	-1.734
36.22	-1.739
36.83	-1.743
37.44	-1.746
38.05	-1.752
38.66	-1.753
39.27	-1.747
39.88	-1.740
40.18	-1.734
40.36	-1.863

References

Carslaw, H. S., and J. C. Jaeger, 1959, Conduction of Heat in Solids: Oxford Univ. Press, London, 386 p.

Gold, L. W., and A. H. Lachenbruch, 1973, Thermal conditions in permafrost--A review of North American literature, in Permafrost--The North American Contribution to the Second International Conference: Natl. Acad. Sci., p. 3-23.

Harrison, W. D., P. D. Miller, and T. E. Osterkamp, 1977, Permafrost beneath the Chukchi Sea - Preliminary report: Alaska Univ. Geophys. Inst. Quart. Rept. (Oct. 31 - Dec. 31, 1976).

Harrison, W. D., and T. E. Osterkamp, 1976, A coupled heat and salt transport model for sub-sea permafrost: Alaska Univ. Geophys. Inst. Rept. UAG R-247, 21 p.

Hopkins, D. M., P. W. Barnes, N. Biswas, J. Cannon, E. Chamberlain, J. Dygas, W. Harrison, A. S. Naidu, D. Nummedal, J. Rogers, P. Sellmann, M. Vigdorchik, W. Wiseman, and T. Osterkamp, 1977, Earth science studies, in Synthesis of scientific studies of the Beaufort Sea: Natl. Atmospheric and Oceanic Administration, in press.

Hunter, J. A. M., A. S. Judge, H. A. MacAulay, R. L. Good, R. M Gagne, and R. A. Burns, 1976, The occurrence of permafrost and frozen subseabottom materials in the southern Beaufort Sea, in Beaufort Sea Tech. Rept. #22: Victoria, B.C., Dept. Environment, 174 p.

Sass, J. H., A. H. Lachenbruch, R. J. Munroe, G. W. Greene, and T. H. Moses, Jr., 1971, Heat flow in the western United States: Jour. Geophys. Research, v. 76, p. 6376-6413.

Sharbatyan, A. A., and P. A. Shumskiy, 1974, Extreme estimations in geothermy and geocryology: U.S. Army Corps Engineers Cold Regions Research and Eng. Lab. Rept. TL 465 [Draft Translation 465].

Terzaghi, K., 1952, Permafrost: Boston Soc. Civil Engineers Jour., v. 39, p. 1-50.